Methylene-Bridged Complexes of Rhodium/Ruthenium as Models for Bimetallic Fischer−Tropsch Catalysts: Comparisons with the Rh/Os and Ir/Ru Analogues

Bryan D. Rowsell, Steven J. Trepanier, Robert Lam,[‡] Robert McDonald,[‡] and Martin Cowie*[,§]

Department of Chemistry, University of Alberta, Edmonton, Alberta, Canada T6G 2G2

Received February 14, 2002

The cationic heterobinuclear complex $[RhRu(CO)_3(\mu\text{-}H)_2(dppm)_2][X]$ (**1**) is prepared by protonation of the monohydride species $[RhRu(CO)_3(\mu\text{-}H)(dppm)_2]$ (dppm = μ-$Ph_2PCH_2PPh_2$; $X^- = BF_4^-, CF_3SO_3^-$). Treatment of **1** with carbon monoxide affords the tetracarbonyl complex ion $[RhRu(CO)_4(dppm)_2][X]$ (**2**), which yields the methylene-bridged product $[RhRu(CO)_4(\mu\text{-}CH)_2(dppm)_2][X]$ (**3**), upon treatment with excess diazomethane at −78 °C. Reaction of **3** with trimethylamine-*N*-oxide results in CO removal, affording the methylene-bridged tricarbonyl species $[RhRu(CO)_3(\mu\text{-}CH)_2(dppm)_2][X]$ (**4**). Although compound **3** is unreactive toward further treatment with CH_2N_2, compound **4** reacts readily with diazomethane, yielding a mixture of uncharacterized products. Compounds **3** and **4** react with PMe_3 to yield $[RhRu(PMe_3)(CO)_3(\mu\text{-}CH)_2(dppm)_2][X]$ (**5**), in which coordination of PMe_3 at the unsaturated Rh center occurs. The structures of compounds **2**, **3**, and **5** have been determined by X-ray methods. Comparisons of the reactivity of compound **3** with that of the analogous Ir/Ru and Rh/Os complexes toward diazomethane are presented.

Introduction

The Fischer−Tropsch (FT) process, in which synthesis gas ($CO + H_2$) is converted into a variety of hydrocarbons, is catalyzed by group 8 and 9 metals.[1] Each of the metals involved has been reported to give rise to different product distributions,[2] and ruthenium is considered to be the most active.[2c,3] The differing reactivities of the different metals and reports of improved selectivities of bimetallic catalysts over monometallic ones in processes such as hydrogenation and alkene isomerization[4,5] suggest a role for bimetallic catalysts in FT chemistry, and reports have appeared of improved product selectivity through the use of mixed Co/Ru FT catalysts.[6]

In the majority of bimetallic catalysts little is understood about the functions of the different metals in the transformations of interest. We have therefore been studying a range of mixed-metal complexes with the goal of developing a better understanding of the roles of the different metals in substrate transformation;[7−26] of particular relevance to FT chemistry are those complexes incorporating combinations of group 8 and 9 metals.[7,10,11,14,16,18−22,24−26] The most promising system studied by us to date is $[RhOs(CO)_4(dppm)_2][X]$ (dppm = μ-$Ph_2PCH_2PPh_2$, X = anion), which can incorporate between one and four methylene units (derived from diazomethane), yielding methylene-bridged (**A**), allyl/methyl (**B**), or butanediyl (**C**) fragments on the metals,

* Corresponding author. E-mail: martin.cowie@ualberta.ca.
‡ X-ray Crystallography Laboratory.
§ Killam Annual Professor 2000/01.

(1) (a) Biloen, P.; Sachtler, W. M. H. *Adv. Catal.* **1981**, *30*, 165. (b) Vander Laan, G. P.; Beenackers, A. A. C. M. *Catal. Rev.-Sci. Eng.* **1999**, *41*, 255. (c) Schulz, H. *Appl. Catal. A* **1999**, *186*, 3. (d) Maitlis, P. M.; Quyoum, R.; Long, H. C.; Turner, M. L. *Appl. Catal. A* **1999**, *186*, 363.
(2) (a) Vannice, M. A. *J. Catal.* **1975**, *37*, 462. (b) Maitlis, P. M.; Long, H. C.; Quyoum, R.; Turner, M. L.; Wang, Z. Q. *J. Chem. Soc., Chem. Commun.* **1996**, 1. (c) Quyoum, R.; Berdini, V.; Turner, M. L.; Long, H. C.; Maitlis, P. M. *J. Catal.* **1998**, *173*, 355.
(3) Maitlis, P. M.; Long, H. C.; Quyoum, R.; Turner, M. L.; Wang, Z. Q. *J. Chem. Soc., Chem. Commun.* **1996**, 1.
(4) Sinfelt, J. H. *Bimetallic Catalysts: Discoveries, Concepts and Applications*; Wiley: New York, 1983; Chapter 2.
(5) da Silva, A. C.; Piotrowski, H.; Mayer, P.; Polborn, K.; Severin, K. *Eur. J. Inorg. Chem.* **2001**, 685.
(6) Iglesia, E.; Soled, S. L.; Fiato, R. A.; Via, G. H. *J. Catal.* **1993**, *143*, 345.
(7) Antonelli, D. M.; Cowie, M. *Organometallics* **1990**, *9*, 1818.
(8) Antonelli, D. M.; Cowie, M. *Inorg. Chem.* **1990**, *29*, 3339.
(9) Antonelli, D. M.; Cowie, M. *Inorg. Chem.* **1990**, *29*, 4039.
(10) Hilts, R. W.; Franchuk, R. A.; Cowie, M. *Organometallics* **1991**, *10*, 304.
(11) Hilts, R. W.; Franchuk, R. A.; Cowie, M. *Organometallics* **1991**, *10*, 1297.
(12) Antonelli, D. M.; Cowie, M. *Organometallics* **1991**, *10*, 2173.
(13) Antonelli, D. M.; Cowie, M. *Organometallics* **1991**, *10*, 2550.
(14) McDonald, R.; Cowie, M. *Inorg. Chem.* **1993**, *32*, 1671.
(15) Wang, L.-S.; McDonald, R.; Cowie, M. *Inorg. Chem.* **1994**, *33*, 3735.
(16) Sterenberg, B. T.; Hilts, R. W.; Moro, G.; McDonald, R.; Cowie, M. *J. Am. Chem. Soc.* **1995**, *117*, 245.
(17) Wang, L.-S.; Cowie, M. *Can. J. Chem.* **1995**, *73*, 1058.
(18) Antwi-Nsiah, F. H.; Oke, O.; Cowie, M. *Organometallics* **1996**, *15*, 1042.
(19) Sterenberg, B. T.; McDonald, R.; Cowie, M. *Organometallics* **1997**, *16*, 2297.
(20) George, D. S. A.; McDonald, R.; Cowie, M. *Organometallics* **1998**, *17*, 2553.
(21) Trepanier, S. J.; Sterenberg, B. T.; McDonald, R.; Cowie, M. *J. Am. Chem. Soc.* **1999**, *121*, 2613.
(22) Oke, O.; McDonald, R.; Cowie, M. *Organometallics* **1999**, *18*, 1629.
(23) Graham, T. W.; VanGastel, F.; McDonald, R.; Cowie, M. *Organometallics* **1999**, *18*, 2177.
(24) George, D. S. A.; Hilts, R. W.; McDonald, R.; Cowie, M. *Organometallics* **1999**, *18*, 5330.
(25) George, D. S. A.; Hilts, R. W.; McDonald, R.; Cowie, M. *Inorg. Chim. Acta* **2000**, *300−302*, 353.
(26) Dell'Anna, M. M.; Trepanier, S. J.; McDonald, R.; Cowie, M. *Organometallics* **2001**, *20*, 88.

10.1021/om020118j CCC: $22.00
Publication on Web 06/22/2002

Table 1. Spectroscopic Data for the Compounds

compd	IR[a,b]	NMR[d,e] δ ($^{31}P\{^1H\}$)[f]	δ (^1H)[g,h]	δ ($^{31}C\{^1H\}$)[h]
$[RhRu(CO)_3(\mu\text{-}H)_2(dppm)_2]$-$[CF_3SO_3]$ (**1a**)	2044 (m), 1970 (br,s)	34.4 (m), 26.2 (dm)	3.87 (m, 4H), −9.65 (m, 2H)	197.0 (t, $^2J_{PC}$ = 12 Hz, 2C), 182.6 (dt, $^2J_{RhC}$ = 75 Hz, $^2J_{PC}$ = 17 Hz, 1C)
$[RhRu(CO)_4(dppm)_2][CF_3SO_3]$ (**2a**)	1987 (m), 1945 (m), 1906 (s)	35.4 (m), 27.1 (dm)	3.9 (m, 4H)	207.6 (t, $^2J_{PC}$ = 13 Hz, 2C), 195.9 (t, $^2J_{PC}$ = 15 Hz, 1C), 179.5 (m, $^2J_{PC}$ = 15 Hz, $^1J_{RhC}$ = 75 Hz, 1C)
$[RhRu(CO)_4(\mu\text{-}CH_2)(dppm)_2]$-$[CF_3SO_3]$ (**3a**)	2043 (m), 2001 (m), 1963 (s), 1802 (m)	35.3 (om)	3.74 (m,2H), 2.80 (m, 2H), 2.43 (m, 2H)	227.4 (m, 1C), 195.4 (dt, $^2J_{PC}$ = 20 Hz, $^1J_{RhC}$ = 66 Hz, 1C), 194.9 (m, 1C), 194.0 (t, $^2J_{PC}$ = 12 Hz, 1C), 48.3 (dpq, $^1J_{RhC}$ = 16 Hz, $^2J_{PC}$ = 5 Hz)
$[RhRu(CO)_3(\mu\text{-}CH_2)(dppm)_2]$-$[CF_3SO_3]$ (**4a**)	2018 (m), 1995 (s), 1957 (s)[c]	30.7 (m), 28.6 (dm)[j]	5.38 (m, 2H), 4.24 (m, 2H), 3.58 (m, 2H)[j]	196.2 (t, $^2J_{PC}$ = 8 Hz, 1C), 195.2 (t, $^2J_{PC}$ = 13 Hz, 1C), 189.1 (dt, $^2J_{PC}$ = 14 Hz, $^1J_{RhC}$ = 68 Hz, 1C), 97.0 (m)[i]
$[RhRu(PMe_3)(CO)_3(\mu\text{-}CH_2)$-$(dppm)_2][CF_3SO_3]$ (**5a**)	1981 (s), 1965 (s), 1919 (s)	26.8 (m), 23.5 (dm), −34.4 (dm)	4.77 (m, 2H), 3.85 (m, 2H), 3.60 (m,2H), 0.70 (d, $^2J_{PH}$ = 10 Hz, 9H)	204.1 (t, $^2J_{PC}$ = 10 Hz, 1C), 199.6 (om, 2C), 90.7 (m)

[a] IR abbreviations: s = strong, m = medium, br = broad. [b] Powder microscope or Nujol mull unless otherwise indicated; in units of cm^{-1}. [c] In THF. [d] NMR abbreviations: s = singlet, d = doublet, t = triplet, m = multiplet, dm = doublet of multiplets, om = overlapping multiplets, br = broad, dt = doublet of triplets, dpq = doublet of pseudo-quintets. [e] NMR data at 25 °C in CD_2Cl_2 unless otherwise indicated; in units of ppm. [f] ^{31}P chemical shifts referenced to external 85% H_3PO_4. [g] Chemical shifts for the phenyl hydrogens not given. [h] ^1H and ^{13}C chemical shifts referenced to TMS. [i] In THF-d_8. [j] In acetone-d_6.

Scheme 1

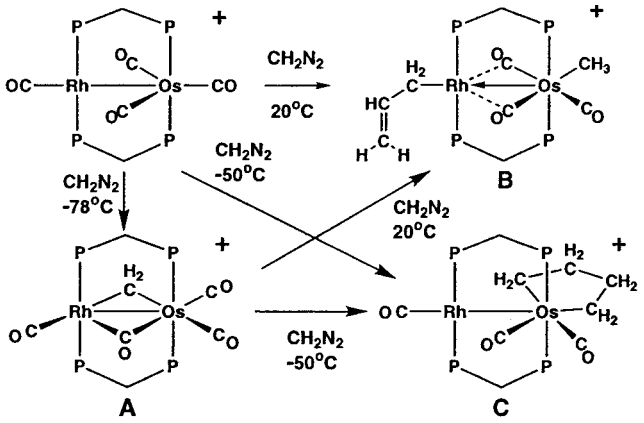

as shown in Scheme 1.[21] The high FT activity of Ru, as well as the rich chemistry of diruthenium complexes in carbon−carbon bond formation,[27] led us to extend the above Rh/Os chemistry to include the Rh/Ru combination of metals, and our preliminary findings on this system are reported herein, as are comparisons with the above Rh/Os system[21] and the related Ir/Ru system.[26] From this comparison we hope to be able to address questions relating to the use of different metal combinations in carbon−carbon bond formation related to FT chemistry.

Experimental Section

General Comments. All solvents were dried (using appropriate desiccants), distilled before use, and stored under a dinitrogen atmosphere. Reactions were performed under an argon atmosphere using standard Schlenk techniques. Diazomethane was generated from Diazald, which was purchased from Aldrich, as was the trimethylphosphine (1 M) solution in THF. The ^{13}C-enriched Diazald was purchased from Cambridge Isotopes, whereas ^{13}CO was purchased from Isotec Inc. The complex $[RhRu(CO)_3(\mu\text{-}H)(dppm)_2]$ was prepared by a published procedure.[7]

The ^1H, $^{13}C\{^1H\}$, and $^{31}P\{^1H\}$ NMR spectra were recorded on a Varian iNova-400 spectrometer operating at 399.8 MHz for ^1H, 161.8 MHz for ^{31}P, and 100.6 MHz for ^{13}C. Infrared spectra were obtained on a Nicolet Magna 750 FTIR spectrometer with a NIC-Plan IR microscope. The elemental analyses were performed by the microanalytical service within the department.

For all the compounds reported, both the triflate ($CF_3SO_3^-$) and tetrafluoroborate (BF_4^-) salts were synthesized through the use of either triflic or tetrafluoroboric acid in the preparation of compound **1**, described below. Compounds having the triflate anion are labeled **a**, whereas those with tetrafluoroborate are labeled **b**. Since the spectroscopic data for the cations were found to be identical, irrespective of anion used, only the syntheses and spectroscopic data (Table 1) for the triflate salts are reported herein. However, crystal structure determinations described are for the tetrafluoroborate salts since our attempts to obtain suitable single crystals of the triflate salts were unsuccessful.

Preparation of Compounds. (a) $[RhRu(CO)_3(\mu\text{-}H)_2(dppm)_2][CF_3SO_3]$ (1a). The compound $[RhRu(CO)_3(\mu\text{-}H)(dppm)_2]$ (100 mg, 0.0945 mmol) was dissolved in 1.0 mL of THF, and 20 mL of diethyl ether was added slowly to produce a cloudy, brown solution. Triflic acid (8.5 μL, 14.1 mg, 0.096 mmol) was added dropwise, causing the precipitation of a yellow solid. The slurry was stirred for 2 h, and the light brown supernatant was removed. The remaining solid was recrystallized from CH_2Cl_2/Et_2O (83% yield). Anal. Calcd for $C_{54}H_{46}F_3O_6P_4RhRuS$: C, 53.70; H, 3.84. Found: C, 53.75; H, 3.81.

(27) See for example: (a) Knox, S. A. R. *J. Organomet. Chem.* **1990**, *400*, 255. (b) Knox, S. A. R. *J. Cluster Sci.* **1992**, *3*, 385. (c) Akita, M.; Hua, R.; Knox, S. A. R.; Moro-oka, Y.; Nakanishi, S.; Yates, M. I. *J. Organomet. Chem.* **1998**, *569*, 71.

(b) [RhRu(CO)$_4$(dppm)$_2$][CF$_3$SO$_3$] (2a). Compound **1a** (100 mg, 0.0810 mmol) was dissolved in 10 mL of CH_2Cl_2 and stirred under a CO atmosphere for 16 h. The orange solution was concentrated to 5 mL, and ether was added slowly to precipitate a yellow solid, which was recrystallized from CH_2Cl_2/Et_2O, washed with 3 × 15 mL of ether, and dried in vacuo (93% yield). Anal. Calcd for $C_{55}H_{44}F_3O_7P_4RhRuS$: C, 53.54; H, 3.59. Found: C, 53.61; H, 3.59.

(c) [RhRu(CO)$_4$(μ-CH$_2$)(dppm)$_2$][CF$_3$SO$_3$]·0.33CH$_2$Cl$_2$ (3a). Compound **2a** (254 mg, 0.206 mmol) was dissolved in 15 mL of CH_2Cl_2 and cooled to −78 °C. Diazomethane, generated from 290 mg of Diazald (1.347 mmol), was passed through the solution vigorously for the duration of CH_2N_2 production. The orange solution was stirred under the diazomethane atmosphere for 1 h, after which the vessel was allowed to warm to room temperature under a stream of argon. The solvent was removed in vacuo, and the orange residue dissolved in 5 mL of CH_2Cl_2 and filtered through Celite (in air). Ether was added dropwise to precipitate orange microcrystals (89% yield). Anal. Calcd for $C_{56.3}H_{46.7}Cl_{0.7}F_3O_7P_4RhRuS$: C, 53.03; H, 3.69; Cl, 1.83. Found: C, 52.86; H, 3.69; Cl, 1.71. The fractional methylene chloride (1/3) of crystallization results from facile desolvation upon removal of crystals from the mother liquor. However, storage under high vacuum did not result in complete solvent loss. Elemental analysis and ^{1}H NMR spectroscopy confirmed the presence of CH_2Cl_2.

(d) [RhRu(CO)$_3$(μ-CH$_2$)(dppm)$_2$][CF$_3$SO$_3$] (4a). A 50 mL portion of acetone was added to a mixture of compound **3a** (126 mg, 0.101 mmol) and Me_3NO (13 mg, 0.173 mmol), resulting in a rapid color change from orange to dark red. The solution was filtered through Celite, and the solvent was removed in vacuo. The residue was recrystallized from acetone/ether/*n*-pentane (1:3:3), washed with 3 × 15 mL of ether, and dried in vacuo (53% yield). The highly air-sensitive nature of **4a** has prevented dependable elemental analysis results.

(e) [RhRu(PMe$_3$)(CO)$_3$(μ-CH$_2$)(dppm)$_2$][CF$_3$SO$_3$] (5a). Method i. Compound **3a** (100 mg, 0.080 mmol) was suspended in 15 mL of THF, and PMe_3 (160 μL of a 1.0 M THF solution, 0.160 mmol) was added. The solution was stirred for 2 h, after which the solvent was removed in vacuo. The yellow residue was recrystallized from CH_2Cl_2/ether, washed with 3 × 15 mL of ether, and dried in vacuo (72% yield). Anal. Calcd for $C_{58}H_{55}F_3O_6P_5RhRuS$: C, 53.75; H, 4.28. Found: C, 53.60; H, 4.27.

Method ii. Compound **4a** (20 mg, 0.0164 mmol) was dissolved in 0.7 mL of CD_2Cl_2 in an NMR tube. PMe_3 (20 μL of a 1.0 M THF solution, 0.020 mmol) was added, and the solution was mixed for 5 min, during which time the color changed from red to yellow. ^{1}H and ^{31}P NMR spectroscopy revealed complete conversion to **5a**.

(f) Reaction of 3 with Excess CH$_2$N$_2$. Compound **3**, as either the $CF_3SO_3^-$ or BF_4^- salt (100 mg, 0.080 mmol), was dissolved in 0.7 mL of CD_2Cl_2 in an NMR tube, and diazomethane, generated from 100 mg (0.464 mmol) of Diazald, was passed through the headspace of the tube. The solution was mixed for 20 min with no noticeable color change. ^{1}H and ^{31}P NMR spectroscopy revealed only the presence of **3** and ethylene.

(g) Reaction of 4 with CO. Compound **4**, as either the $CF_3SO_3^-$ or BF_4^- salt (20 mg, 0.0164 mmol), was placed in an NMR tube, and 0.7 mL of CD_2Cl_2 was added. Addition of carbon monoxide caused the solution to turn from red to orange-yellow immediately. ^{31}P and ^{1}H NMR spectroscopy confirmed complete conversion to compound **3**.

(h) Reaction of 4 with Excess CH$_2$N$_2$. Compound **4**, as either the $CF_3SO_3^-$ or BF_4^- salt (100 mg, 0.080 mmol), was dissolved in 0.7 mL of CD_2Cl_2 in an NMR tube, and diazomethane, generated from 100 mg (0.464 mmol) of Diazald, was passed through the headspace of the tube. The solution was mixed for 20 min with no noticeable color change. ^{1}H and ^{31}P NMR spectroscopy revealed the formation of at least three new uncharacterized products.

X-ray Data Collection. Data for all compounds were collected on a Bruker P4/RA/SMART 1000 CCD diffractometer[28] using Mo Kα radiation at −80 °C. Yellow crystals of [RhRu(CO)$_4$(dppm)$_2$][BF$_4$] (**2b**) were obtained from slow diffusion of Et_2O into a concentrated CH_2Cl_2 solution of the compound. Orange crystals of [RhRu(CO)$_4$(μ-CH$_2$)(dppm)$_2$][BF$_4$] (**3b**) were obtained by slow diffusion of Et_2O into a concentrated CH_2Cl_2 solution of the compound. Although the triflate salt (**3a**) contained CH_2Cl_2 of crystallization, no solvent is present in crystals of the BF_4^- salt. Yellow crystals of [RhRu(PMe$_3$)(CO)$_3$(μ-CH$_2$)(dppm)$_2$][BF$_4$] (**5b**) were obtained from slow diffusion of Et_2O into a concentrated CH_2Cl_2 solution of the compound. Unit cell parameters for the compounds were obtained from a least-squaresd refinement of the setting angles of 4710 reflections for **2b**, 4386 reflections for compound **3b**, and 6861 reflections for compound **5b** from the data collection. Space groups for **2b** and **5b** were determined to be $P2_1/c$, and that of **3b** was found to be $I2/a$ (a nonstandard setting of $C2/c$). The data for all compounds were corrected for absorption by use of the SADABS procedure.

Structure Solution and Refinement. All structures were solved using direct methods (SHELXS-86),[29] and refinement was completed using the program SHELXL-93.[30] Hydrogen atoms were assigned positions on the basis of the geometries of their attached carbon atoms and were given thermal parameters 20% larger than those of attached carbons. Compound **2b** is disordered about the inversion center at (0, 0, 0), such that the metal sites are each composed of 1/2 occupancy of each metal (Rh/Ru). The only other atoms affected by the disorder are C(2) and C(3), which each appear at 1/2 occupancy at inversion-related sites. The BF_4^- ion was also disordered about the inversion center at (0, 1/2, 0). Despite the disorder, all atom positions were resolved and least-squares refinement proceeded well.

In compound **5b** both metals have similar coordination environments, so the identification of Rh or Ru is not obvious. However, interchanging the scattering factors for the two metals resulted in an obvious enlargement of the thermal parameters for the incorrectly labeled Rh atom and a contraction of those for Ru, indicating that too few electrons were at the former site and too many at the latter. At the same time, the residuals upon convergence for this model are marginally worse ($R_1 = 0.0521$, $wR_2 = 0.1300$) than for the correct model ($R_1 = 0.0506$, $wR_2 = 0.1200$). Both effects indicate that the original model, having the labeling reported, is correct. This model also agrees with the spectroscopic data (vide infra). Crystallographic data for compounds **2b**, **3b**, and **5b** are given in Table 2.

Results and Compound Characterization

The methylene-bridged complex [RhRu(CO)$_4$(μ-CH$_2$)(dppm)$_2$][X] (**3**) has been prepared from [RhRu(CO)$_3$(μ-H)(dppm)$_2$] by the series of reactions shown in Scheme 2. Protonation of this monohydride, using either triflic acid or tetrafluoroboric acid, yields [RhRu(CO)$_3$(μ-H)$_2$(dppm)$_2$][X] (X = SO_3CF_3 (**1a**), BF_4 (**1b**)), as the respective triflate or tetrafluoroborate salts (in subsequent discussions a compound number without **a** or **b** designation means that identical results were obtained with both $CF_3SO_3^-$ and BF_4^- salts). Both hydride ligands in **1** are chemically equivalent and appear as a multiplet at δ −9.55 in the ^{1}H NMR spectrum due to coupling to

(28) Programs for diffractometer operation, data reduction, and absorption correction were those supplied by Bruker.
(29) Sheldrick, G. M. *Acta Crystallogr.* **1990**, *A46*, 467.
(30) Sheldrick, G. M. *SHELXL-93*: Program for Crystal Structre Determination; University of Göttingen: Göttingen, Germany, 1993.

Table 2. Crystallographic Data for Compounds 2b, 3b, and 5b

	$[RhRu(CO)_4(dppm)_2][BF_4]$ (**2b**)	$[RhRu(CO)_4(\mu\text{-}CH_2)(dppm)_2][BF_4]$ (**3b**)	$[RhRu(PMe_3)(CO)_3(\mu\text{-}CH_2)(dppm)_2][BF_4]\cdot 2CH_2Cl_2$ (**5b**)
formula	$C_{54}H_{44}BF_4O_4P_4RhRu$	$C_{55}H_{46}BF_4O_4P_4RhRu$	$C_{59}H_{59}BCl_4F_4O_3P_5RhRu$
fw	1171.56	1185.59	1403.50
cryst dimens, mm	0.39 × 0.24 × 0.12	0.63 × 0.13 × 0.08	0.38 × 0.16 × 0.07
cryst syst	monoclinic	monoclinic	monoclinic
space group	$P2_1/c$ (No. 14)	$I2/a$ (No. 15)	$P2_1/c$ (No. 14)
a, Å	11.5763(6)[a]	42.754(5)[b]	20.3808(13)[c]
b, Å	12.7597(7)	10.240(1)	12.7481(9)
c, Å	17.4006(10)	23.590(3)	23.2397(14)
β, deg	101.663(10)	90.455(2)	91.4953(16)
V, Å^3	2516.8(2)	10327(2)	6036.0(7)
Z	2	8	4
d_{calcd}, g cm^{-3}	1.546	1.525	1.544
μ, mm^{-1}	0.815	0.796	0.889
diffractometer	Bruker P4/RA/SMART 1000 CCD[d]	Bruker P4/RA/SMART 1000 CCD[d]	Bruker P4/RA/SMART 1000 CCD[d]
radiation (λ, Å)	graphite-monochromated Mo Kα (0.710 73)	graphite-monochromated Mo Kα (0.710 73)	graphite-monochromated Mo Kα (0.710 73)
T, °C	−80	−80	−80
scan type	ϕ rotations (0.3°)/ω scans (0.3°) (30 s exposures)	ϕ rotations (0.3°)/ω scans (0.3°) (30 s exposures)	ϕ rotations (0.3°)/ω scans (0.3°) (30 s exposures)
2θ(max), deg	52.76	52.82	52.82
no. of unique reflns	5141	10 526	12 333
no. of observns (NO)	4489	8180	7751
no. of variables (NV)	340	626	703
range of abs corr factors	0.909−0.742	0.939−0.634	0.956−0.730
residual density, e/Å^3	0.59 to −0.36	1.48 to −0.70	1.21 to −1.10
R_1 ($F_o^2 > 2\sigma(F_o^2)$)[e]	0.0255	0.0415	0.0506
wR_2 (all data)	0.0690	0.1051	0.1200
GOF (s)[f]	1.028	1.010	0.951

[a] Cell parameters obtained from least-squares refinement of 4710 centered reflections. [b] Cell parameters obtained from least-squares refinement of 4386 centered reflections. [c] Cell parameters obtained from least-squares refinement of 6861 centered reflections. [d] Programs for diffractometer operation, data reduction, and absorption were those supplied by Bruker. [e] $R_1 = \sum||F_o| - |F_c||/\sum|F_o|$; $wR_2 = [\sum w(F_o^2 - F_c^2)^2/\sum w(F_o^4)]^{1/2}$. [f] $S = [\sum w(F_o^2 - F_c^2)^2/(n-p)]^{1/2}$ (n = number of data; p = number of parameters varied; $w = [\sigma^2(F_o^2) + (a_oP)^2 + a_1P]^{-1}$, where $P = [\max(F_o^2,0) = 2F_c^2]/3$. For **2b** $a_o = 0.0368$ and $a_1 = 1.1895$; for **3b** $a_o = 0.0587$ and $a_1 = 5.1691$; for **5b** $a_o = 0.0527$ and $a_1 = 0.00$.

Scheme 2

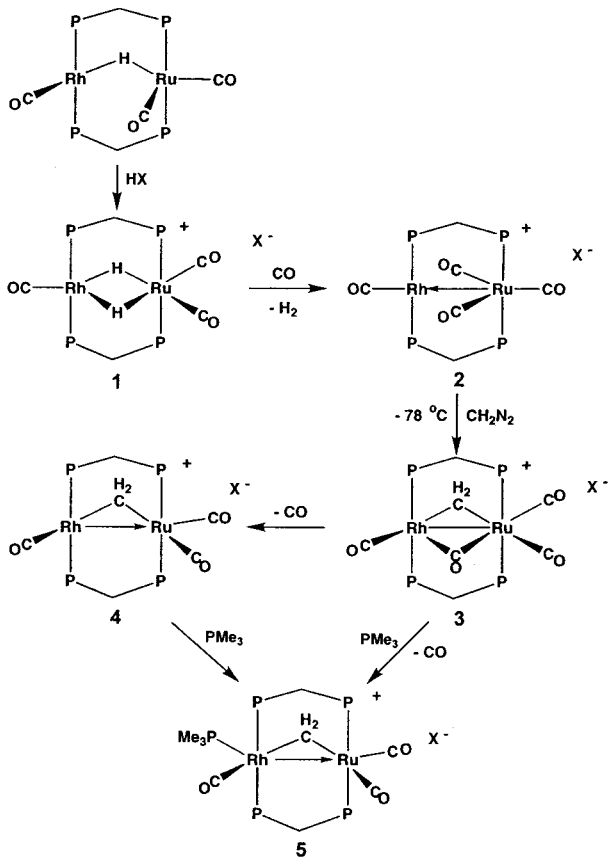

four phosphorus and one ^{103}Rh nuclei. The $^{31}P\{^1H\}$ NMR spectrum of **1** is characteristic of an AA′BB′X spin system found in these types of dppm-bridged heterobinuclear systems with the Rh-bound end of the diphosphine (δ 26.2) being slightly upfield from the Ru-bound end (δ 34.4). In the $^{13}C\{^1H\}$ NMR spectrum two carbonyl resonances are observed in a 2:1 intensity ratio. The more intense signal at δ 197.0 corresponds to the pair of chemically equivalent, Ru-bound carbonyls, while the other, at δ 182.6, displays 75 Hz coupling to Rh and corresponds to the terminal carbonyl on this metal.

Reaction of **1** with carbon monoxide results in elimination of H_2 and accompanying coordination of CO, affording the cationic tetracarbonyl $[RhRu(CO)_4(dppm)_2][X]$ (**2**), which displays three carbonyl resonances in the $^{13}C\{^1H\}$ NMR spectrum in a 1:1:2 intensity ratio at 25 °C. The high-field resonance (δ 179.5), showing coupling of 75 Hz to Rh, is identified as that terminally bound to this metal, the intermediate signal at δ 195.9 is a triplet, displaying coupling to the pair of Ru-bound ^{31}P nuclei, while the low-field resonance (also a triplet) integrating as two carbonyls corresponds to the two Ru-bound CO ligands that are bent toward Rh. The slight downfield shift of these carbonyls is presumed to result from the interaction with the adjacent Rh, as has previously been observed.[20] However, it is clear that any interaction of these carbonyls with Rh must be weak since no coupling to this nucleus is observed in the $^{13}C\{^1H\}$ NMR spectrum, and the IR spectrum of **2** shows only terminal carbonyls.

The solid-state structure of **2** confirms what is proposed based on spectroscopic data, and this structure is shown for the cation in Figure 1. About Rh, the geometry is square planar in which the Ru occupies one of the coordination sites. If the metal−metal bond is

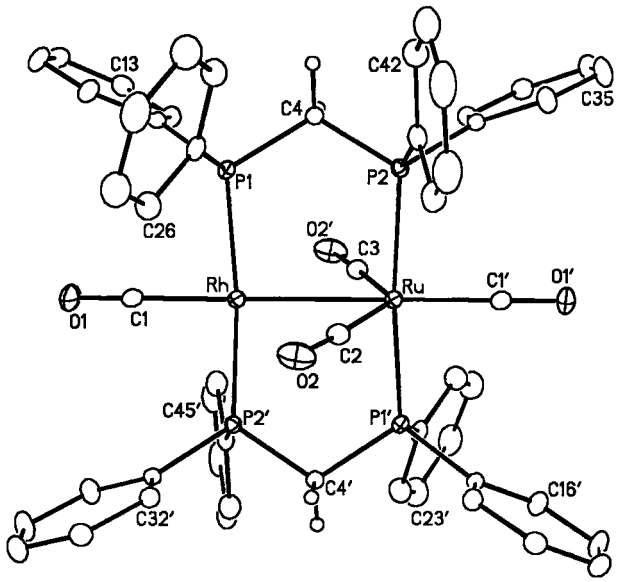

Figure 1. Perspective view of the $[RhRu(CO)_4(dppm)_2]^+$ complex cation of **2b** showing the atom-labeling scheme. Non-hydrogen atoms are represented by Gaussian ellipsoids at the 20% probability level. The methylene hydrogen atoms are shown with arbitrarily small thermal parameters, while the dppm phenyl hydrogens are not shown. Primed atoms are related to unprimed ones by inversion symmetry. Only one of the disordered structures is shown. For an explanation of the disorder see the Experimental Section.

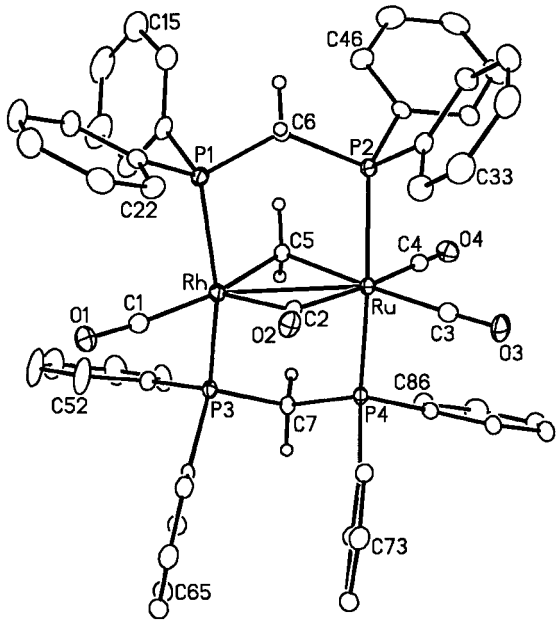

Figure 2. Perspective view of the $[RhRu(CO)_4(\mu\text{-}CH_2)(dppm)_2]^+$ cation of **3b** showing the atom-labeling scheme. Thermal parameters are as described for Figure 1.

ignored, the geometry at Ru is best described as trigonal bipyramidal, in which the C(2)−Ru−C(3) angle, which is bisected by the metal−metal bond, has opened up to 131.7(2)° with a corresponding decrease in the other carbonyl angles to 113.6(1)° and 114.7(2)°. The Rh−Ru distance (2.7870(3) Å) is normal for a single bond showing substantial contraction of the metal−metal separation compared to the intraligand P−P separation (3.0176(6) Å). The X-ray structure also shows that C(2)O(2) and C(3)O(2′), although aimed toward Rh, remain terminally bound to Ru. The long Rh−C(2) and Rh−C(3) distances (2.665(4) and 2.678(4) Å) confirm that any interaction between Rh and these carbonyls must be extremely weak.

Reaction of **2** with diazomethane at −78 °C generates the methylene-bridged product $[RhRu(CO)_4(\mu\text{-}CH_2)(dppm)_2][X]$ (**3**) quantitatively, as shown in Scheme 2. The ^1H NMR spectrum reveals the resonance for the μ-CH_2 group as a pseudo-quintet at δ 2.43 with essentially equal coupling to all four ^{31}P nuclei. No coupling of the methylene protons to Rh is obvious. This signal can be differentiated from the dppm methylene protons (at δ 3.74 and 2.80) by using broad-band ^{31}P decoupling, resulting in a collapse of the metal-bound methylene signal to a singlet, while the dppm-methylene signals collapse to the expected AB quartet. It is important to point out that selective ^{31}P decoupling, in which only one of the two ^{31}P resonances is decoupled, is not possible in some of these compounds, due to the close proximity of the two resonances. In compound **3** the two sets of resonances are superimposed.

The $^{13}C\{^1H\}$ NMR spectrum of a ^{13}CO-enriched sample of **3** shows the expected four resonances, with the lowest-field signal (δ 227.4) being attributed to the bridging CO ligand. Broad-band ^{31}P-decoupling experiments show that this carbonyl also displays a 25 Hz coupling to Rh, consistent with a strong semibridging interaction. The signal at δ 195.4 appears as a doublet of triplets with coupling to the Rh nucleus of 66 Hz, clearly indicating that it is Rh-bound. The remaining two carbonyl signals are due to the pair that are terminally bound to Ru. The ^{13}C resonance for the bridging methylene group ($^{13}CH_2$-enriched sample) appears as a doublet of pseudo-quintets at δ 48.3, displaying 16 Hz coupling to Rh and 5 Hz coupling to all phosphorus nuclei. The IR spectrum helps confirm the carbonyl bonding assignment, showing three terminal CO bands (2043, 2001, and 1963 cm^{-1}) and one for the semibridging CO (1802 cm^{-1}).

The structure of **3b** was confirmed by an X-ray structure determination, and the complex cation is shown in Figure 2, with important bond lengths and angles given in Table 4. This compound has a doubly bridged "A-frame" structure, in which the metals are bridged by the methylene group and a carbonyl on opposite faces of the "$RhRuP_4$" plane. The Rh−Ru separation (2.9114(5) Å) is longer than a normal single bond involving these metals and can be compared to that observed in **2b**, which is in the normal range of such bonds. However, this metal−metal separation is still significantly less than the intraligand P−P separations (3.205(1) and 3.004(1) Å), indicating a mutual attraction of the metals. If the Rh−Ru bond is ignored, the geometry about Ru can be viewed as octahedral, while Rh has a tetragonal pyramidal geometry in which the apical site is occupied by the bridging carbonyl. This carbonyl can be considered as semibridging, although the asymmetry in the angles about the carbonyl carbon (Rh−C(2)−O(2) = 130.4(3)°, Ru−C(2)−O(2) = 141.1(3)°) is not as great as usually observed.[31] Surprisingly, the asymmetry in metal−carbonyl bond lengths is the opposite of what one might expect with the Ru−C(2) distance (2.155(4) Å) being *longer* than Rh−C(2) (2.021-

(31) Crabtree, R. H.; Lavin, M. *Inorg. Chem.* **1986**, *25*, 805.

Table 3. Selected Distances and Angles for Compound 2b

(i) Distances (Å)

atom1	atom2	distance	atom1	atom2	distance
Rh	Ru	2.7870(3)	Ru	C(3)	1.950(4)
Rh	P(1)	2.3368(5)	P(1)	P(2)	3.0176(6)[b]
Rh	P(2′)[a]	2.3346(5)	P(1)	C(4)	1.834(2)
Rh	C(1)	1.885(2)	P(2)	C(4)	1.834(2)
Rh	C(2)	2.665(4)[b]	O(1)	C(1)	1.126(3)
Rh	C(3)	2.678(4)[b]	O(2)	C(2)	1.218(4)
Ru	C(2)	1.969(4)	O(2′)	C(3)	1.224(4)

(ii) Angles (deg)

atom1	atom2	atom3	angle	atom1	atom2	atom3	angle
Ru	Rh	P(1)	92.41(1)	P(2)	Ru	C(3)	88.3(1)
Ru	Rh	P(2′)	93.20(1)	C(1′)	Ru	C(2)	113.6(1)
Ru	Rh	C(1)	179.13(8)	C(1′)	Ru	C(3)	114.7(2)
P(1)	Rh	P(2′)	173.78(2)	C(2)	Ru	C(3)	131.7(2)
P(1)	Rh	C(1)	87.47(7)	Rh	P(1)	C(4)	113.17(6)
P(2′)	Rh	C(1)	86.96(7)	Ru	P(2)	C(4)	113.56(6)
Rh	Ru	C(2)	65.6(1)	Rh	C(1)	O(1)	179.7(3)
Rh	Ru	C(3)	66.1(1)	Ru	C(2)	O(2)	175.3(3)
P(1′)	Ru	C(2)	89.7(1)	Ru	C(3)	O(2′)	174.8(3)
P(1′)	Ru	C(3)	91.5(1)	P(1)	C(4)	P(2)	110.7(1)
P(2)	Ru	C(2)	95.1(1)				

[a] Primed atoms related to unprimed ones by the crystallographic inversion center at (0, 0, 0). [b] Nonbonded distance.

Table 4. Selected Distances and Angles for Compound 3b

(i) Distances (Å)

atom1	atom2	distance	atom1	atom2	distance
Rh	Ru	2.9114(5)	Ru	C(5)	2.213(3)
Rh	P(1)	2.305(1)	P(1)	P(2)	3.205(1)[a]
Rh	P(3)	2.351(1)	P(1)	C(6)	1.840(3)
Rh	C(1)	1.900(4)	P(2)	C(6)	1.853(4)
Rh	C(2)	2.021(3)	P(3)	P(4)	3.004(1)[a]
Rh	C(5)	2.089(3)	P(3)	C(7)	1.835(3)
Ru	P(2)	2.382(1)	P(4)	C(7)	1.835(3)
Ru	P(4)	2.382(1)	O(1)	C(1)	1.137(4)
Ru	C(2)	2.155(4)	O(2)	C(2)	1.164(4)
Ru	C(3)	1.927(4)	O(3)	C(3)	1.139(4)
Ru	C(4)	1.913(4)	O(4)	C(4)	1.136(4)

(ii) Angles (deg)

atom1	atom2	atom3	angle	atom1	atom2	atom3	angle
Ru	Rh	P(1)	96.24(2)	P(2)	Ru	C(5)	84.2(1)
Ru	Rh	P(3)	94.68(2)	P(4)	Ru	C(2)	93.7(1)
Ru	Rh	C(1)	142.8(1)	P(4)	Ru	C(3)	91.4(1)
Ru	Rh	C(2)	47.7(1)	P(4)	Ru	C(4)	86.3(1)
Ru	Rh	C(5)	49.24(9)	P(4)	Ru	C(5)	90.7(1)
P(1)	Rh	P(3)	156.12(3)	C(2)	Ru	C(3)	92.1(1)
P(1)	Rh	C(1)	92.6(1)	C(2)	Ru	C(4)	172.7(1)
P(1)	Rh	C(2)	95.3(1)	C(2)	Ru	C(5)	88.9(1)
P(1)	Rh	C(5)	83.3(1)	C(3)	Ru	C(4)	95.2(2)
P(3)	Rh	C(1)	91.5(1)	C(3)	Ru	C(5)	177.6(1)
P(3)	Rh	C(2)	107.8(1)	C(4)	Ru	C(5)	83.8(1)
P(3)	Rh	C(5)	87.9(1)	Rh	P(1)	C(6)	112.5(1)
C(1)	Rh	C(2)	95.6(2)	Ru	P(2)	C(6)	115.4(1)
C(1)	Rh	C(5)	167.9(1)	Rh	P(3)	C(7)	112.0(1)
C(2)	Rh	C(5)	96.1(1)	Ru	P(4)	C(7)	113.2(1)
Rh	Ru	P(2)	90.82(2)	Rh	C(1)	O(1)	173.0(3)
Rh	Ru	P(4)	86.78(2)	Rh	C(2)	Ru	88.3(1)
Rh	Ru	C(2)	43.94(9)	Rh	C(2)	O(2)	130.4(3)
Rh	Ru	C(3)	135.6(1)	Ru	C(2)	O(2)	141.1(3)
Rh	Ru	C(4)	128.8(1)	Ru	C(3)	O(3)	175.7(3)
Rh	Ru	C(5)	45.65(9)	Ru	C(4)	O(4)	178.2(3)
P(2)	Ru	P(4)	174.72(3)	Rh	C(5)	Ru	85.1(1)
P(2)	Ru	C(2)	87.8(1)	P(1)	C(6)	P(2)	120.4(2)
P(2)	Ru	C(3)	93.6(1)	P(3)	C(7)	P(4)	109.9(2)
P(2)	Ru	C(4)	91.6(1)				

[a] Nonbonded distance.

(3) Å). Usually in semibridging carbonyls the shorter distance is associated with the metal that forms the more linear carbonyl arrangement (Ru in this case). The bridging methylene group is also unsymmetrically bridged, again being more tightly bound to Rh (Rh−C(5) = 2.089(3) Å, Ru−C(5) = 2.213(3) Å). It should be

noted, however, that in **3b** all metal−ligand bonds are shorter for Rh than for Ru. This may be a consequence of the differences in coordination geometry, with greater repulsions giving rise to longer bonds at the more crowded Ru center.

A comparison with two other closely related compounds, $[RhOs(CO)_4(\mu\text{-}CH_2)(dppm)_2][BF_4]$[32] and $[IrRu(CO)_4(\mu\text{-}CH_2)(dppm)_2][BF_4]$,[26] is of interest. The Rh/Ru and Rh/Os compounds have almost identical geometries with only extremely minor variations in bond lengths and angles, so will not be discussed further at this point. However the Ir/Ru analogue has more substantial differences, although these differences are still not large. The major difference results from the bonding of the bridging carbonyl, which for the Ir/Ru compound is essentially symmetrically bridged. As a result, the Ir−C(2) and Ru−C(2) distances in the Ir/Ru analogue are comparable at 2.033(8) and 2.072(8) Å, respectively, in contrast to the more asymmetric Rh−C(2) and Ru−C(2) distances (2.021(3), 2.155(4) Å) in **3b**. In addition, the angles at the bridging carbonyl group in the Ir/Ru analogue (Ir−C(2)−O(2) = 134.4(7)°, Ru−C(2)−O(2) = 137.1(7)°) are also indicative of a more symmetrically bridging carbonyl. Accompanying the slight change in carbonyl bonding from **3b** to the Ir/Ru analogue is a corresponding shortening of the metal−metal bond (to 2.8650(7) Å in the Ir/Ru species) and a corresponding bending back of the terminally bound iridium carbonyl (C(5)−Ir−C(1) = 161.7(5)°) compared to the angle of 167.9(1)° in **3b**. We will attempt to address the possible significance of these differences later.

Addition of excess diazomethane to compound **3** does not afford any new organometallic products, although ethylene is observed in both the ^1H and $^{13}C\{^1H\}$ NMR spectra. Surprisingly, when $^{13}CH_2N_2$ is used in the reaction with **3**, no ^{13}C incorporation into the methylene bridge of **3** is observed. The only product of ^{13}C incorporation is $^{13}C_2H_4$. After extended exposure of **3** to CH_2N_2, unreacted **3** is the only complex observed.

Reaction of **3** with trimethylamine-*N*-oxide results in carbonyl loss to yield the tricarbonyl product $[RhRu(CO)_3(\mu\text{-}CH_2)(dppm)_2][X]$ (**4**). The ^1H NMR spectrum of **4** shows the metal-bound methylene unit at δ 5.38. As was the case for **3**, broad-band ^{31}P decoupling clearly allows us to distinguish the bridging μ-CH_2 from the dppm methylenes (δ 4.24 and 3.58). The $^{13}C\{^1H\}$ NMR spectrum of a ^{13}CO-enriched sample of **4** shows the expected three carbonyl resonances, with the high-field signal appearing as a doublet of triplets ($^1J_{RhC} = 68$ Hz), confirming that this carbonyl is terminally bound to Rh, and the remaining two signals appear as triplets, corresponding to the two carbonyls that are bound to Ru. In a $^{13}CH_2$-enriched sample of **4** the methylene carbon appears as a multiplet at δ 97.0 in the ^{13}C NMR spectrum. The IR spectrum of **4** shows three terminal CO stretches (ν_{CO}: 1931, 1966, and 1992 cm^{-1}). As expected, reaction of **4** with carbon monoxide regenerates **3**. Loss of a carbonyl from **3** necessitates a subtle change in the nature of the Rh−Ru bonding; in **4** we propose that the coordinative unsaturation that results from CO loss is alleviated by formation of a dative Rh→Ru bond from the filled d_{z^2} orbital on the square-planar Rh(+1) center.

(32) Trepanier, S. J.; Cowie, M. Unpublished results.

Whereas the methylene-bridged compound **3** is not transformed into other species in the presence of additional diazomethane at ambient temperature, the tricarbonyl **4** reacts rapidly at temperatures as low as −78 °C. Unfortunately, even at −78 °C, the reaction of **4** with CH_2N_2 yields a mixture of at least three products, which have not yet been identified.

Compounds **3** and **4** both react with PMe_3, affording the phosphine adduct, $[RhRu(PMe_3)(CO)_3(\mu\text{-}CH_2)(dppm)_2][X]$ (**5**). The $^{31}P\{^1H\}$ NMR spectrum of **5** shows low-field multiplets for the Rh- and Ru-bound ends of the diphosphine ligands (δ 23.5 and 26.8, respectively) and a high-field doublet of multiplets at δ −34.4, corresponding to the PMe_3 group. The large rhodium coupling ($^1J_{RhP} = 120$ Hz) for the PMe_3 group clearly identifies that this ligand is bound to Rh. In the related Ir/Ru complex, $[IrRu(PMe_3)(CO)_3(\mu\text{-}CH_2)(dppm)_2][BF_4]$, the PMe_3 group is again bound to the group 9 metal.[26] As was observed in the Ir/Ru compound, the ^{31}P nucleus of PMe_3 in **5** shows coupling to both ends of the diphosphine ligands (in this case, the Rh- and Ru-bound ends). Unfortunately, the proximity of the two signals is not conducive to selective decoupling experiments, so the magnitude of the coupling to the two sets of dppm ^{31}P nuclei could not be determined. In related compounds, the PMe_3 group on one metal can display comparable or *greater* coupling to the ^{31}P nuclei on the *adjacent* metal than to those on the same metal.[22,26] The $^1H\{^{31}P\}$ NMR spectrum of **5** confirms that the signal at δ 3.60 is due to the bridging methylene group. A ^{13}C NMR spectrum of a ^{13}CO-enriched sample of **5** shows only two carbonyl resonances in a 1:2 ratio. The high-field signal is actually comprised of two overlapping multiplets (corresponding to the Rh-bound and one Ru-bound carbonyl), from which coupling information could not be extracted. The ^{13}C resonance for the bridging methylene group appears at δ 90.7, but coupling information again could not be extracted due to poor signal-to-noise ratio in the spectrum derived from an unenriched sample.

The X-ray structure of the cationic complex of **5b** is shown in Figure 3, with relevant bond lengths and angles given in Table 5. As indicated in the $^{31}P\{^1H\}$ NMR investigation and confirmed in this X-ray study, the PMe_3 group is bound to Rh, giving rise to an almost symmetrical ligand arrangement in which both metals have, in addition to the bridging groups, two terminally bound two-electron-donor ligands; Rh is bound to the PMe_3 group and one carbonyl, while Ru has two carbonyls. As in compound **3b**, the Rh−Ru separation in **5b** (2.8952(6) Å) is longer than a normal single bond (cf. compound **2b**: Rh−Ru = 2.7870(3) Å) but is again less than the intraligand P−P separation (3.002(2), 2.954(2) Å), suggesting attraction of the metals. In addition, a metal−metal bond (in some form) is needed to satisfy the valence electron counts of the metals. Two bonding extremes can be considered. If the positive charge of the complex is localized on Ru, the metals have Rh(+1) and Ru(+2) oxidation states (μ-CH_2 viewed as a dianionic ligand) and a dative Rh→Ru bond is required to give Ru its preferred 18e configuration. However, if the positive charge is localized on Rh, the oxidation states are Rh(+2) and Ru(+1) with a conventional metal−metal bond. We prefer the former formulation, as

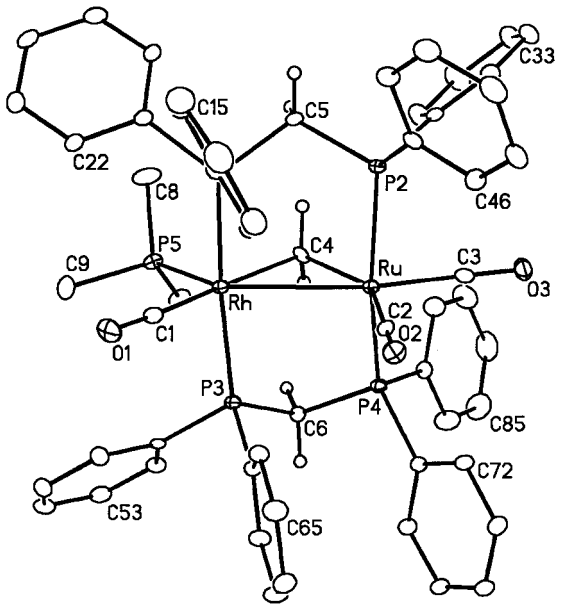

Figure 3. Perspective view of the $[RhRu(PMe_3)(CO)_3(\mu\text{-}CH_2)(dppm)_2]^+$ cation of **5b** showing the atom-labeling scheme. Thermal parameters are as described for Figure 1.

diagrammed in Scheme 2, in line with the common oxidation states of these metals.

The PMe_3 group influences the structure in a number of subtle ways. Its steric size causes the diphosphines bound to Rh to bend away from it and also causes a similar distortion at Ru, giving rise to P(1)−Rh−P(3) and P(2)−Ru−P(4) angles of 165.55(5)° and 161.04(4)°, respectively—significantly distorted from the idealized 180° value. This PMe_3 group also appears to influence two of the metal−carbonyl distances. Although carbonyls C(1)O(1) and C(2)O(2) occupy similar positions on each metal, the former appears to be more tightly bound (Rh−C(1) = 1.900(5) Å, Ru−C(2) = 1.934(5) Å), presumably a consequence of greater π back-donation resulting from the basic PMe_3 group. Of some surprise is that the shortest metal−carbonyl distance is that of Ru−C(3) (1.860(5) Å). It is becoming recognized that electronic effects can be transmitted through a metal−metal bond;[33] in this case it appears that electron donation by the PMe_3 group to Rh can be transmitted via the Rh−Ru bond to C(3)O(3), which lies almost opposite this bond. This transmission of electron density from Rh to Ru can be rationalized considering the above bonding formulation, in which a dative Rh→Ru bond is proposed. Electron donation to Rh by the basic PMe_3 group would result in Rh being a better donor to Ru.

Although compound **5** is isoelectronic with **3**, resulting from replacement of one carbonyl group by the PMe_3 moiety, their geometries are significantly different. In **3** the Rh center has only one terminally bound ligand (a carbonyl), whereas in **5** Rh has two terminally bound groups. The presence of two terminal ligands bound to Rh in **5** is unexpected based on steric arguments, since the larger PMe_3 group should favor the carbonyl being pushed toward Ru, as observed in **3**, in which it is bridging. However, it appears that the terminal carbonyl is favored electronically since in this bonding mode it can more effectively function to remove electron density from Rh that is donated by the PMe_3 group. It is also interesting that the ligand arrangement on the metals is not symmetric. The "$Rh(CO)(PMe_3)$" fragment has been twisted away from the metal−metal bond more than the corresponding "$Ru(CO)_2$" fragment. As a result, the PMe_3 group lies significantly off the Rh−Ru vector (Ru−Rh−P(5) = 129.91(4)°), whereas the carbonyl C(3)O(3) is close to this vector (Rh−Ru−C(3) = 164.8(2)°). It appears that this relative twisting about the metal centers allows the phenyl rings of the dppm ligands to fit in the interligand gaps in a gear-wheel arrangement. As inspection of Figure 3 shows that phenyl rings 1 and 6 are aimed into the cavity between the metals, opening up the Ru−Rh−C(1) angle, while phenyl ring 8 is aimed between C(3)O(3) and the bridging methylene group. Other phenyl groups are aiming between other ligand combinations or are twisted (phenyl rings 2 and 5) to avoid contacts with the PMe_3 group.

It is notable that for the three methylene-bridged compounds reported (**3**, **4**, and **5**) there is a correlation between the ^1H and ^{13}C chemical shifts for the methylene groups (a high-field ^1H chemical shift corresponds to a high-field signal in the ^{13}C NMR spectrum and vice versa). Unfortunately, however, these NMR data are not helpful in establishing whether there is a metal−metal bond. It has been noted[34] that for metal−metal bonded species the ^1H NMR resonance for a bridging methylene group generally lies in the range δ 5−11, whereas the ^{13}C resonance is also low-field, in the range δ 100−210. Both sets of resonances for compounds **3** and **5** are upfield from these ranges, although the Rh−CH_2−Ru angle in each compound (85.1(1)°, 85.5(2)°) lies within the range (73−88°) given for metal−metal bonded species.[35] As noted earlier, we consider these complexes to be metal−metal bonded despite their long metal−metal separations.

Discussion

The bridging methylene unit has been shown to be a pivotal fragment in FT chemistry and has been implicated in carbon−carbon bond formation through a number of proposed pathways.[1a,36−38] Following our success with coupling of up to four methylene fragments promoted by a Rh/Os compound,[21] we turned to the Rh/Ru combination of metals in order to determine the effect of substituting Os by the more labile Ru.[39] However, much of the chemistry reported herein is inconsistent with this interpretation and necessitates a consideration of not only Ru-for-Os replacement but

(33) (a) Cowie, M.; Vasapollo, G.; Sutherland, B. R.; Ennett, J. P. *Inorg. Chem.* **1986**, *25*, 2648. (b) Sola, E.; Torres, F.; Jimenez, M. V.; López, J. A.; Ruiz, S. E.; Lahoz, F. J.; Elduque, A.; Oro, L. A. *J. Am. Chem. Soc.* **2001**, *123*, 11925.

(34) Puddephatt, R. J. *Polyhedron* **1988**, *7*, 767.

(35) Herrmann, W. A. *Adv. Organomet. Chem.* **1982**, *20*, 159.

(36) Kaminsky, M. P.; Winograd, N.; Geoffroy, G. L.; Vannice, M. A. *J. Am. Chem. Soc.* **1986**, *108*, 1315.

(37) (a) Brady, R. C.; Pettit, R. *J. Am. Chem. Soc.* **1980**, *102*, 6181. (b) Brady, R. C.; Pettit, R. *J. Am. Chem. Soc.* **1981**, *103*, 1287.

(38) (a) Maitlis, P. M.; Long, H. C.; Quyoum, R.; Turner, M. L.; Wang, Z.-Q. *Chem. Commun.* **1996**, 1. (b) Long, H. C.; Turner, M. L.; Fornasiero, P.; Kaspar, J.; Graziani, M.; Maitlis, P. M. *J. Catal.* **1997**, *167*, 172.

(39) Huheey, J. E.; Keiter, E. A.; Keiter, R. L. *Inorganic Chemistry: Principles of Structure and Reactivity*, 4th ed.; Harper Collins: New York, 1993.

Table 5. Selected Distances and Angles for Compound 5b

(i) Distances (Å)

atom1	atom2	distance	atom1	atom2	distance
Rh	Ru	2.8952(6)	P(1)	C(5)	1.833(5)
Rh	P(1)	2.340(1)	P(2)	C(5)	1.822(5)
Rh	P(3)	2.322(1)	P(3)	P(4)	2.954(2)[a]
Rh	P(5)	2.400(1)	P(3)	C(6)	1.830(4)
Rh	C(1)	1.900(5)	P(4)	C(6)	1.836(5)
Rh	C(4)	2.148(4)	P(5)	C(7)	1.826(5)
Ru	P(2)	2.352(1)	P(5)	C(8)	1.822(5)
Ru	P(4)	2.370(1)	P(5)	C(9)	1.809(6)
Ru	C(2)	1.934(5)	O(1)	C(1)	1.136(6)
Ru	C(3)	1.860(5)	O(2)	C(2)	1.130(5)
Ru	C(4)	2.117(5)	O(3)	C(3)	1.164(6)
P(1)	P(2)	3.002(2)[a]			

(ii) Angles (deg)

atom1	atom2	atom3	angle	atom1	atom2	atom3	angle
Ru	Rh	P(1)	88.90(4)	P(2)	Ru	C(4)	86.8(1)
Ru	Rh	P(3)	85.04(4)	P(4)	Ru	C(2)	100.5(2)
Ru	Rh	P(5)	129.91(4)	P(4)	Ru	C(3)	84.7(2)
Ru	Rh	C(1)	125.8(2)	P(4)	Ru	C(4)	84.3(1)
Ru	Rh	C(4)	46.8(1)	C(2)	Ru	C(3)	95.6(2)
P(1)	Rh	P(3)	165.55(5)	C(2)	Ru	C(4)	147.3(2)
P(1)	Rh	P(5)	99.17(5)	C(3)	Ru	C(4)	117.1(2)
P(1)	Rh	C(1)	85.2(2)	Rh	P(1)	C(5)	114.3(2)
P(1)	Rh	C(4)	91.6(1)	Ru	P(2)	C(5)	114.4(2)
P(3)	Rh	P(5)	94.77(5)	Rh	P(3)	C(6)	113.1(2)
P(3)	Rh	C(1)	87.7(2)	Ru	P(4)	C(6)	113.1(2)
P(3)	Rh	C(4)	93.8(1)	Rh	P(5)	C(7)	116.9(2)
P(5)	Rh	C(1)	104.2(2)	Rh	P(5)	C(8)	119.1(2)
P(5)	Rh	C(4)	83.4(1)	Rh	P(5)	C(9)	115.8(2)
C(1)	Rh	C(4)	172.2(2)	C(7)	P(5)	C(8)	98.4(3)
Rh	Ru	P(2)	92.99(4)	C(7)	P(5)	C(9)	101.5(3)
Rh	Ru	P(4)	93.28(4)	C(8)	P(5)	C(9)	102.0(3)
Rh	Ru	C(2)	99.6(2)	Rh	C(1)	O(1)	177.2(5)
Rh	Ru	C(3)	164.8(2)	Ru	C(2)	O(2)	178.1(5)
Rh	Ru	C(4)	47.7(1)	Ru	C(3)	O(3)	178.5(5)
P(2)	Ru	P(4)	161.04(4)	Rh	C(4)	Ru	85.5(2)
P(2)	Ru	C(2)	96.1(2)	P(1)	C(5)	P(2)	110.5(2)
P(2)	Ru	C(3)	84.5(2)	P(3)	C(6)	P(4)	107.3(2)

[a] Nonbonded distance.

also the effects of different *combinations* of metals (i.e., Rh/Ru vs Rh/Os and Ir/Ru), as will be discussed.

The transformations from $[RhRu(CO)_3(\mu\text{-}H)(dppm)_2]$ to $[RhRu(CO)_4(\mu\text{-}CH_2)(dppm)_2][X]$ (**3**), as shown in Scheme 2, are not surprising and parallel previous work done with the Rh/Os[21] and Ir/Ru[26] combinations of metals. What is surprising is the subsequent lack of reactivity of **3** with diazomethane, compared to the analogous Rh/Os compound, which reacts readily under similar conditions (Scheme 1). Although **3** and its Ir/Ru analogue do not incorporate additional methylene groups from diazomethane, they do generate ethylene. Labeling studies in both compounds show that little or none of the labeled methylene from diazomethane becomes incorporated into the complexes nor does any of the metal-bridged methylene group become incorporated into the ethylene. In contrast, labeling studies for the Rh/Os compound $[RhOs(CO)_4(\mu\text{-}CH_2)(dppm)_2][X]$ have shown that ethylene formation results from coupling of the metal-bridged methylene group with a second methylene group generated by diazomethane, presumably by diazomethane activation at the unsaturated Rh center. In this Rh/Os system, ethylene is either liberated from the complex or subsequent methylene incorporation occurs, yielding the C_3- and C_4-containing species shown in Scheme 1.[21] The failure of $^{13}CH_2$-labeled **3** to transfer any of the label to the ethylene produced shows that a different mechanism for ethylene formation is operating, although what this mechanism is remains unclear.

In hopes of obtaining clues about the differing reactivities of the methylene-bridged Rh/Os complex compared to those of Rh/Ru (**3**) and Ir/Ru, we compared their solid-state structures. However, the closely comparable structural parameters for these compounds (particularly the Rh/Ru and Rh/Os analogues) gave no obvious clue to the reactivity differences. Looking back at the transformation of $[RhOs(CO)_4(\mu\text{-}CH_2)(dppm)_2]^+$ into either $[RhOs(CH_2CH{=}CH_2)(CH_3)(CO)_3(dppm)_2]^+$ or $[RhOs(CH_2)_4(CO)_3(dppm)_2]^+$ (Scheme 1), it was clear that carbonyl loss accompanied these interesting examples of C−C bond formation. However, in the previous study[21] we had not established the stage at which carbonyl loss occurred or its relationship to the methylene-coupling reactions. To test the effect of carbonyl loss in the Rh/Ru system, the removal of one carbonyl by Me_3NO was effected, yielding the tricarbonyl species $[RhRu(CO)_3(\mu\text{-}CH_2)(dppm)_2][X]$ (**4**). Unlike the methylene-bridged tetracarbonyl precursor (**3**), which remains unaffected by additional CH_2N_2, compound **4** reacts readily, yielding a mixture of products. Although we have been unable to characterize any of these products, the reactivity of **4** with diazomethane suggests that CO loss is pivotal in subsequent incorporation of methylene

Table 6. Comparison of Selected Structural Parameters for the Compounds $[MM'(CO)_4(\mu\text{-}CH_2)(dppm)_2][BF_4]$ (MM′ = RhOs, RhRu, IrRu)[a]

	MM′		
	RhOs[21]	RhRu (**3**)[c]	IrRu[26]
	(a) Bond Lengths (Å)		
M−M′ [b]	2.9413(4)	2.9114(5)	2.8650(7)
M′−C(2)	2.157(4)	2.155(4)	2.072(8)
M−C(2)	2.027(4)	2.021(3)	2.033(8)
M′−C(5)	2.210(4)	2.213(3)	2.305(12)
M−C(5)	2.088(4)	2.089(3)	2.045(11)
	(b) Angles (deg)		
M′−C(2)−O(2)	141.7(3)	141.1(3)	137.1(7)
M−C(2)−O(2)	128.9(3)	130.4(3)	134.4(7)
C(5)−M−C(1)	169.1(2)	167.9(1)	161.7(5)

[a] The number scheme used for all compounds is that used for compound **3** in Figure 2. [b] M = Rh, Ir; M′ = Ru, Os. [c] This work.

groups, leading to methylene coupling. It seemed, therefore, that the clue to the reactivity differences in the Rh/Ru and Rh/Os compounds may lie in their abilities to lose CO upon reaction with diazomethane. Two closely related extremes can be envisioned for methylene-bridged tetracarbonyl complexes of Rh/Ru and Rh/Os as diagrammed for **D** and **E** (dppm groups above and below the plane of the drawing are omitted). In structure **E**, Rh is coordinatively unsaturated, whereas in the metal−metal bonded **D**, both metals have 18e configurations. Structure **E** should therefore be more susceptible to substrate addition, which might induce CO loss as diagrammed in **F**. The coordinative saturation at Rh, resulting from substrate (L) addition, can lead to dative-bond formation to M (Ru or Os) assisting in the labilization of a carbonyl. In keeping with this proposal, the reaction of **3** with PMe_3 yields the substitution product **5**, which appears to have resulted from PMe_3 attack as diagrammed in structure **F**. That PMe_3 reacts readily with **3**, whereas diazomethane does not, is presumably a result of the greater nucleophilicity of the former. With these ideas in mind, we looked back at the structures of $[RhRu(CO)_4(\mu\text{-}CH_2)(dppm)_2][BF_4]$ (**3b**) and the Rh/Os and Ir/Ru analogues to determine their relationship to the extreme structures shown in **D** and **E**. Clearly, the transition from **E** to **D** is accompanied by a shortening of the metal−metal separation and by a change in the M−C−O angle from 180° to near 140° as this carbonyl assumes a bridging position. A comparison of structural parameters for the three methylene-bridged compounds under discussion is given in Table 6.

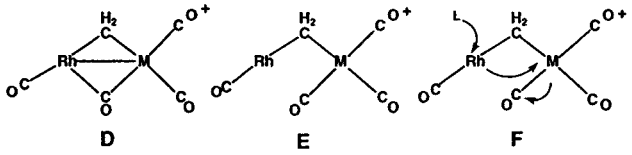

On the basis of the parameters given in Table 6, it is clear that the Ir/Ru compound is close to the symmetrically bridged carbonyl extreme, **D** (numbering scheme as in Figure 2). In this compound the Ir−C(2)−O(2) and the Ru−C(2)−O(2) angles are comparable, as are the Ir−C(2) and Ru−C(2) distances. As shown in structure **D**, the symmetrical carbonyl bridge is accompanied by a metal−metal bond; consequently this Ir/Ru compound has the shortest metal−metal distance of the three. In addition, as the carbonyl group (C(2)−O(2)) moves to a bridging arrangement, the C(5)−Rh−C(1) or C(5)−Ir−C(1) angle should decrease from 180° expected in structure **E** as interaction of this metal with C(2)−O(2) increases. Consistent with this argument, this angle is smallest for the Ir/Ru structure. Although, as noted earlier, a comparison of **3b** and the Rh/Os analogue was not very helpful since both structures are very similar, it is useful to compare them in the context of the above discussion. So although the Rh−C(2) and M−C(2) distances (M = Ru, Os) are not significantly different in the two structures, other parameters given in Table 6 show a clear trend. Therefore, the differences between the Rh−C(2)−O(2) and M−C(2)−O(2) angles in the two structures are 10.7° (Rh/Ru) and 12.8° (Rh/Os), with the Rh/Ru structure tending slightly toward the symmetric extreme. This tendency is supported by a shorter Rh−M bond and a less linear C(5)−Rh−C(1) angle in the Rh/Ru compound, both of which suggest a tendency toward a symmetrically bridged structure. These parameters, taken together, suggest that the Rh/Os compound tends most toward the structure type **E**, which should, based on the assessment diagrammed in **F**, be more prone to diazomethane coordination and subsequent CO loss. This tendency toward a symmetrically bridged carbonyl for the Rh/Ru compound compared to Rh/Os is also supported by the solution NMR studies. In **3** the semibridging carbonyl displays a somewhat larger coupling to Rh (25 Hz) compared to that observed (22 Hz) for the Rh/Os analogue,[32] suggesting stronger binding to Rh in the former.

Although we recognize that the structural differences between **3** and its Rh/Os analogue are slight and are susceptible to overinterpretation, the most important aspect of these arguments is the recognition that a number of factors associated with *both* metals, including the nature of the metal−metal bonding, are responsible for the reactivity of binuclear complexes.

Acknowledgment. We thank the Natural Sciences and Engineering Research Council of Canada (NSERC) and the University of Alberta for financial support of this research and the NSERC for funding the P4/RA/SMART 1000 CCD diffractometer. M.C. thanks the University of Alberta and the Killam Trusts for a Killam Annual Research Professorship.

Supporting Information Available: Tables of X-ray experimental details, atomic coordinates, interatomic distances and angles, anisotropic thermal parameters, and hydrogen parameters for compounds **2b**, **3b**, and **5b**. This material is available free of charge via the Internet at http://pubs.acs.org.

OM020118J